

SUPPORTING INFORMATION

**Homoleptic Uranium and Lanthanide Phosphinodiboranates**

Anastasia V. Blake,<sup>†,[a]</sup> Taylor V. Fetrow,<sup>†,[a]</sup> Zachary J. Theiler,<sup>[a]</sup> Bess Vlasisavljevič,<sup>\*,[b]</sup>  
Scott R. Daly<sup>\*,[a]</sup>

<sup>[a]</sup>Department of Chemistry, The University of Iowa, E331 Chemistry Building, Iowa City, IA  
52242-1294

<sup>[b]</sup>Department of Chemistry, University of South Dakota, 414 E. Clark Street, Vermillion, SD  
57069

E-mail: [Bess.Vlasisavljevič@usd.edu](mailto:Bess.Vlasisavljevič@usd.edu); [scott-daly@uiowa.edu](mailto:scott-daly@uiowa.edu)

<sup>†</sup>Equal contributions.

## 1. Experimental Section

**General Considerations.** All reactions were carried out using standard glovebox or Schlenk techniques under an N<sub>2</sub> atmosphere. All glassware was heated overnight at 150 °C and allowed to cool under vacuum before use. Pentane, Et<sub>2</sub>O, and THF were dried and degassed using a Pure Process Technologies Solvent Purification System. Anhydrous 1,4-dioxane (99%) was purchased from Sigma Aldrich, dried over 3 Å molecular sieves, and distilled under vacuum before use. Deuterated solvents were dried over activated 3 Å molecular sieves and deoxygenated by freeze-pump-thaw methods. UI<sub>3</sub>(1,4-dioxane)<sub>1.5</sub> and K(H<sub>3</sub>B<sup>1</sup>Bu<sub>2</sub>PBH<sub>3</sub>) were synthesized as reported previously.<sup>[1]</sup> All other chemicals were purchased from commercial vendors and used as received.

<sup>1</sup>H NMR data were recorded on a Bruker AVANCE-300 instrument operating at 300 MHz or on a Bruker DRX-400 instrument operating at 400 MHz. <sup>13</sup>C NMR data were collected on a Bruker DRX-400 instrument operating at 101 MHz. <sup>11</sup>B NMR data were collected on a Bruker DRX-400 instrument operating at 128 MHz. Chemical shifts are reported in δ units relative to residual solvent peaks (<sup>1</sup>H, <sup>13</sup>C) or BF<sub>3</sub>·Et<sub>2</sub>O (<sup>11</sup>B). Attempts to collect <sup>31</sup>P NMR data on **1** – **3** and <sup>13</sup>C NMR data on **1** and **3** were unsuccessful due to unresolved peak broadening from sample paramagnetism and quadrupolar coupling with <sup>10</sup>B and <sup>11</sup>B. Microanalytical data (CHN) were collected using an EAI CE-440 Elemental Analyzer in the UI Department of Chemistry. IR spectra were acquired on a Thermo Scientific Nicolet iS5 in an N<sub>2</sub>-filled glovebox using an attenuated reflection (ATR) accessory. Melting points were determined in sealed capillaries using a REACH MP Device.

**Caution!** Depleted uranium (primarily U-238) is a weak α-emitter (4.197MeV) with a 4.47 x 10<sup>9</sup> half-life. All manipulations should be carried out in an approved fume hood or glovebox.

**U<sub>2</sub>(H<sub>3</sub>B<sup>1</sup>Bu<sub>2</sub>PBH<sub>3</sub>)<sub>6</sub>, (1).** K(H<sub>3</sub>B<sup>1</sup>Bu<sub>2</sub>PBH<sub>3</sub>) (101 mg, 0.584 mmol) in Et<sub>2</sub>O (5 mL) was added to a stirring solution of UI<sub>3</sub>(1,4-dioxane)<sub>1.5</sub> (119 mg, 0.158 mmol) in Et<sub>2</sub>O (3 mL). Stirring the mixture for 12 h formed a dark red solution in the presence of a white precipitate. The mixture was filtered through celite, layered with pentane, and stored at -30 °C. After four days, dark burgundy needles formed at the bottom of the vial. Yield: 18 mg (15 %). MP > 260 °C. Anal. Calcd for C<sub>48</sub>H<sub>144</sub>B<sub>12</sub>P<sub>6</sub>U<sub>2</sub>: C, 38.10; H, 9.59. Found C, 38.08; H, 9.55. (EA data was collected after leaving the crystals under dynamic vacuum overnight to remove solvent in the lattice.) <sup>1</sup>H NMR (400 MHz, toluene-*d*<sub>8</sub>): δ 0.38 (br d, *J* = 8 Hz, 18 H, C(CH<sub>3</sub>)<sub>3</sub>, **1**), 1.73 (br s, 36 H, C(CH<sub>3</sub>)<sub>3</sub>, **1**), 72.7 (br s, 6 H, BH<sub>3</sub>, **1**), 94.6 (br s, 12 H, BH<sub>3</sub>, **1**), 100.6 (br s, BH<sub>3</sub>, **1a**). <sup>11</sup>B NMR (128 MHz, toluene-*d*<sub>8</sub>): δ 120.8 (br s, BH<sub>3</sub>, **1**), 180.5 (br s, BH<sub>3</sub>, **1a**), 301.3 (br s, BH<sub>3</sub>, **1**). IR (ATR, cm<sup>-1</sup>): 2981 (m), 2961 (s), 2947 (m), 2926 (w), 2898 (m), 2867 (m), 2424 (m), 2383 (w), 2349 (w), 2240 (sh), 2224 (vs), 1475 (m), 1461 (sh), 1390 (m), 1366 (s), 1240 (vs), 1182 (s), 1128 (w), 1062 (vs), 1048 (m), 1021 (vs), 936 (m), 896 (w), 816 (vs).

**Nd<sub>2</sub>(H<sub>3</sub>B<sup>1</sup>Bu<sub>2</sub>PBH<sub>3</sub>)<sub>6</sub>, (2).** K(H<sub>3</sub>B<sup>1</sup>Bu<sub>2</sub>PBH<sub>3</sub>) (120 mg, 0.570 mmol) in Et<sub>2</sub>O (5 mL) was added to a stirring suspension of NdI<sub>3</sub> (99 mg, 0.19 mmol) in Et<sub>2</sub>O (1 mL). The blue mixture was stirred at RT for 3 h and filtered. Slow evaporation of the filtrate over several days yielded purple blocks

and blue needles of **2**. XRD studies revealed that the blocks and needles had the same unit cell. Yield: 52 mg (42%). MP > 260 °C. Anal. Calcd for C<sub>48</sub>H<sub>144</sub>B<sub>12</sub>P<sub>6</sub>Nd<sub>2</sub>·Et<sub>2</sub>O: C, 44.62; H, 11.09. Found C, 44.55; H, 11.20. <sup>1</sup>H NMR (400 MHz, toluene-*d*<sub>8</sub>): δ 1.23 (br d, *J* = 5.7 Hz, 18 H, C(CH<sub>3</sub>)<sub>3</sub>, **2**), 1.66 (br s, 36 H, C(CH<sub>3</sub>)<sub>3</sub>, **2**), 2.71 (br s, 54 H, C(CH<sub>3</sub>)<sub>3</sub>, **2a**) 76.7 (br m, 12 H, BH<sub>3</sub>, **2**), 78.9 (br m, 6 H, BH<sub>3</sub>, **2**), 84.3 (br m, 18 H, BH<sub>3</sub>, **2a**). <sup>11</sup>B NMR (128 MHz, toluene-*d*<sub>8</sub>): δ 76.7 (br m, BH<sub>3</sub>, **2**), 78.8 (br m, BH<sub>3</sub>, **2a**), 84.1 (br m, BH<sub>3</sub>, **2**). <sup>13</sup>C NMR (101 MHz, C<sub>6</sub>D<sub>6</sub>): δ 31.9 (s, C(CH<sub>3</sub>)<sub>3</sub>, **2**), 32.2 (s, C(CH<sub>3</sub>)<sub>3</sub>, **2**), 33.8 (br s, C(CH<sub>3</sub>)<sub>3</sub>, **2a**). The C(CH<sub>3</sub>)<sub>3</sub> resonances were not observed. IR (ATR, cm<sup>-1</sup>): 2981 (m), 2962 (m), 2946 (m), 2926 (w), 2898 (m), 2867 (m), 2426 (s), 2350 (m), 2255 (sh), 2226 (vs), 1475 (m), 1464 (sh), 1447 (sh), 1396 (sh), 1391 (m), 1366 (s), 1241 (s), 1203 (sh), 1180 (s), 1128 (m), 1063 (vs), 1050 (sh), 1021 (vs), 934 (w), 815 (vs).

**Er<sub>2</sub>(H<sub>3</sub>BP<sup>t</sup>Bu<sub>2</sub>BH<sub>3</sub>)<sub>6</sub>, (3).** K(H<sub>3</sub>BP<sup>t</sup>Bu<sub>2</sub>BH<sub>3</sub>) (105 mg, 0.608 mmol) in Et<sub>2</sub>O (5 mL) was added to a suspension of ErI<sub>3</sub> (99.5 mg, 0.182 mmol) in Et<sub>2</sub>O (3 mL). Stirring the mixture for 12 h resulted in pink solution and a white precipitate. The mixture was filtered through celite and evaporated to dryness under vacuum. The solid was extracted out of hot pentane (50 mL), filtered, and evaporated to dryness under vacuum to yield analytically-pure light pink product. Single crystals were subsequently grown from concentrated pentane solutions. Yield: 42 mg (34 %). MP > 260 °C. Anal. Calcd for C<sub>48</sub>H<sub>144</sub>B<sub>12</sub>P<sub>6</sub>Er<sub>2</sub>·C<sub>5</sub>H<sub>12</sub>: C, 44.09; H, 10.89. Found: C, 44.03; H, 10.37. <sup>1</sup>H NMR (400 MHz, toluene-*d*<sub>8</sub>): -1.16 (br s, 54 H, C(CH<sub>3</sub>)<sub>3</sub>, **3a**), -181.1 (br s, BH<sub>3</sub>, **3a**). <sup>11</sup>B NMR (128 MHz, toluene-*d*<sub>8</sub>): -281.1 (br s, BH<sub>3</sub>, **3a**). IR (ATR, cm<sup>-1</sup>): 2962 (m), 2947 (sh), 2897 (m), 2866 (m), 2429 (m), 2357 (m), 2343 (sh), 2258 (m), 1475 (m), 1459 (sh), 1390 (m), 1366 (s), 1261 (br), 1183 (m), 1065 (s), 1020 (vs), 934 (m), 900 (m), 888 (sh), 872 (sh), 816 (vs).

**Single-crystal X-ray diffraction studies.** Single crystals obtained from Et<sub>2</sub>O/pentane (**1**), Et<sub>2</sub>O (**2**), or pentane (**3**) were mounted on a MiTeGen micromount with ParatoneN oil. The data were collected as described previously.<sup>[2]</sup> The structures were solved with Direct Methods (SHELXT or SHELXS) and least squares refinement (SHELXL) confirmed the location of the non-hydrogen atoms.<sup>[3]</sup> All hydrogen atom positions were idealized and were initially allowed to ride on the attached carbon or boron atoms with B-H distances fixed at 1.20 Å. Anisotropic temperature factors for all non-hydrogen atoms were included at the last refinement. Some of the carbon displacement parameters on the *tert*-butyl groups in **1** and **2** were restrained to be equal to produce satisfactory ellipsoids. The C-C bond distances in **1** and **2** were also restrained to be equal with an effective standard deviation of 0.01 Å. An Et<sub>2</sub>O molecule in the crystal lattice of **1** and **2** was refined with an SOF = 0.5. The C-C and C-O bond distances were fixed at 1.54 ± 0.01 Å and 1.43 ± 0.01 Å. The displacement parameters of the disordered components and Et<sub>2</sub>O were constrained to produce satisfactory ellipsoids. Solvent in the structure of **3** was too disordered to model, so a solvent mask was applied. HKL reflections with error/esd values ±10.0 were omitted from the models. Structure solution, refinement, and generation of publication figures were performed with Olex2.<sup>[4]</sup> The data collection and refinement details are provided in Table S1.

**Table S1.** Single-crystal X-ray diffraction data for  $\text{U}_2(\text{H}_3\text{BP}^i\text{Bu}_2\text{BH}_3)_6 \cdot \frac{1}{2}\text{Et}_2\text{O}$  (**1**· $\frac{1}{2}\text{Et}_2\text{O}$ ),  $\text{Nd}_2(\text{H}_3\text{BP}^i\text{Bu}_2\text{BH}_3)_6 \cdot \frac{1}{2}\text{Et}_2\text{O}$  (**2**· $\frac{1}{2}\text{Et}_2\text{O}$ ), and  $\text{Er}_2(\text{H}_3\text{BP}^i\text{Bu}_2\text{BH}_3)_6$  (**3**).

	<b>1</b> · $\frac{1}{2}\text{Et}_2\text{O}$	<b>2</b> · $\frac{1}{2}\text{Et}_2\text{O}$	<b>3</b>
formula	$\text{C}_{52}\text{H}_{154}\text{B}_{12}\text{OP}_6\text{U}_2$	$\text{C}_{52}\text{H}_{154}\text{B}_{12}\text{OP}_6\text{Nd}_2$	$\text{C}_{48}\text{H}_{144}\text{B}_{12}\text{Er}_2\text{P}_6$
FW (g mol <sup>-1</sup> )	1587.40	1399.83	1371.69
crystal system	monoclinic	monoclinic	monoclinic
space group	P2 <sub>1</sub> /n	P2 <sub>1</sub> /n	P2 <sub>1</sub> /n
a (Å)	15.0395(15)	15.0204(15)	14.7928(15)
b (Å)	12.0078(12)	11.9884(12)	12.1704(12)
c (Å)	24.766(2)	24.771(2)	24.504(2)
$\alpha$ (°)	90	90	90
$\beta$ (°)	90.114(5)	90.050(5)	91.557(5)
$\gamma$ (°)	90	90	90
volume (Å <sup>3</sup> )	4472.5(7)	4460.5(7)	4409.9(7)
Z	2	2	2
$\rho_{\text{calc}}$ (g cm <sup>-3</sup> )	1.179	1.042	1.033
$\mu$ (mm <sup>-1</sup> )	3.750	1.285	2.022
F(000)	1616	1488	1436
R(int)	0.0436	0.0955	0.1561
data/restraints/parameters	8185/107/244	9136/77/262	8646/0/282
GOF	1.137	1.040	1.060
$R_1 [I > 2\sigma(I)]^a$	0.0510	0.0612	0.0770
wR <sub>2</sub> (all data) <sup>b</sup>	0.1386	0.1817	0.2011
Ext. Coeff	none	none	none
Largest Peak/Hole (e·Å <sup>-3</sup> )	1.555/-1.173	1.558/-1.241	2.289/-1.201
Temp (K)	190(1)	190(1)	190(1)

<sup>a</sup> $R_1 = \sum |F_o| - |F_c| / \sum |F_o|$  for reflections with  $F_o^2 > 2 \sigma(F_o^2)$ .

<sup>b</sup> $wR_2 = [\sum w(F_o^2 - F_c^2)^2 / \sum (F_o^2)^2]^{1/2}$  for all reflections.

**Table S2.** Select bond distances (Å) and angles (deg) from the TPSS-D3 geometry optimizations.

	Monomer			Dimer		
	M-B Distance	B-B Distance	B-P-B Angle	M-B Distance	B-B Distance	B-P-B Angle
<b>U</b>	2.764	3.257	111.9	2.909	3.079	104.6
	2.764	3.104	105.5	2.841	3.070	104.1
	2.818	3.109	105.7	2.884	3.109 <sup>a</sup>	107.9 <sup>a</sup>
	2.836			2.840	3.116 <sup>a</sup>	108.1 <sup>a</sup>
	2.840			2.602 <sup>a</sup>	3.043	103.0
	2.814			2.622 <sup>a</sup>	3.043	103.0
				2.625 <sup>a</sup>		
				2.607 <sup>a</sup>		
				2.862		
				2.876		
				2.872		
				2.862		
	<b>Nd</b>	2.804	3.142	107.1	2.848	3.126
2.804		3.158	107.8	2.817	3.097	105.3
2.788		3.192	109.2	2.851	3.163 <sup>a</sup>	110.2 <sup>a</sup>
2.820				2.834	3.160 <sup>a</sup>	110.7 <sup>a</sup>
2.783				2.633 <sup>a</sup>	3.077	104.5
2.775				2.624 <sup>a</sup>	3.150	107.7
				2.645 <sup>a</sup>		
				2.634 <sup>a</sup>		
				2.859		
				2.842		
				2.837		
				2.817		
<b>Er</b>		2.727	3.074	104.0	2.728	3.019
	2.697	3.083	104.4	2.751	3.038	102.6
	2.708	3.047	102.8	2.775	3.214 <sup>a</sup>	113.0 <sup>a</sup>
	2.706			2.707	3.236 <sup>a</sup>	114.1 <sup>a</sup>
	2.732			2.536 <sup>a</sup>	3.123	106.3
	2.720			2.672 <sup>a</sup>	3.020	101.8
				2.743 <sup>a</sup>		
				2.496 <sup>a</sup>		
				2.703		
				3.201		
				2.722		
				2.715		

<sup>a</sup>Indicates distances and angles associated with bridging <sup>t</sup>Bu-PDB ligands

## 2. Experimental Spectra

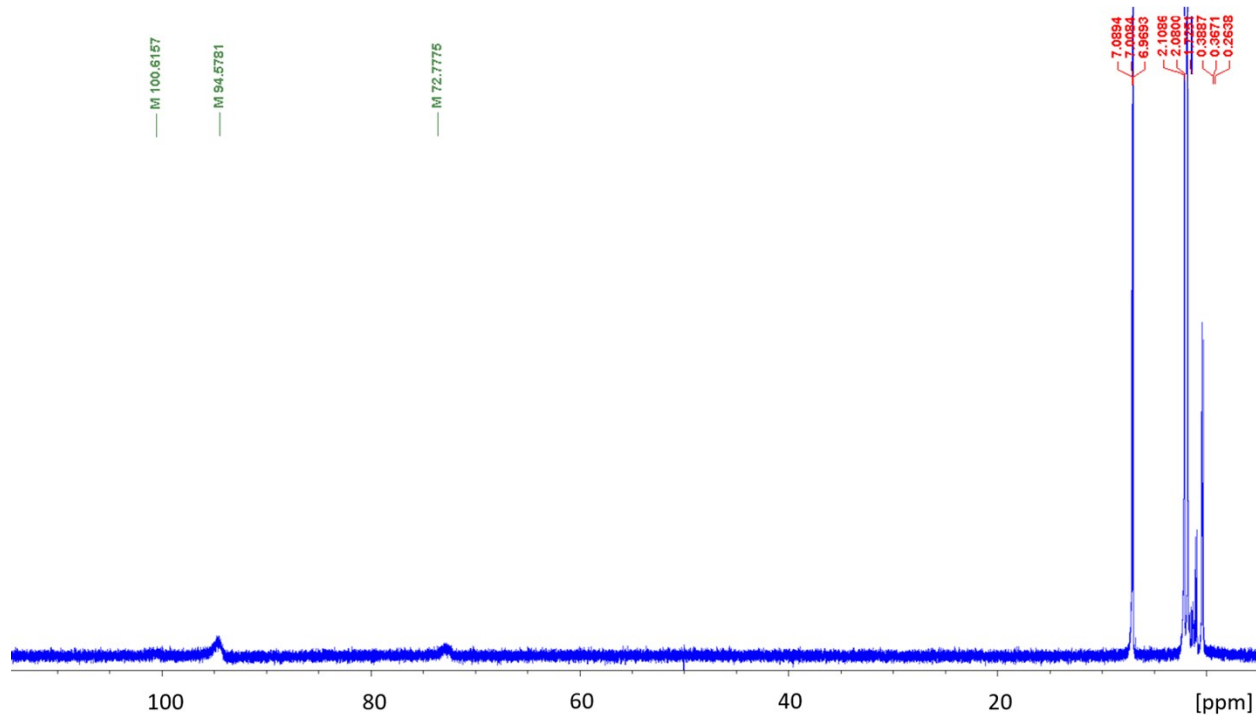


**Figure S1.** <sup>1</sup>H NMR full spectrum of U<sub>2</sub>(H<sub>3</sub>BP'Bu<sub>2</sub>BH<sub>3</sub>)<sub>6</sub> (1) in toluene-*d*<sub>8</sub> at 20 °C. Data collected after leaving the crystals under dynamic vacuum overnight to remove solvent in the crystal lattice.

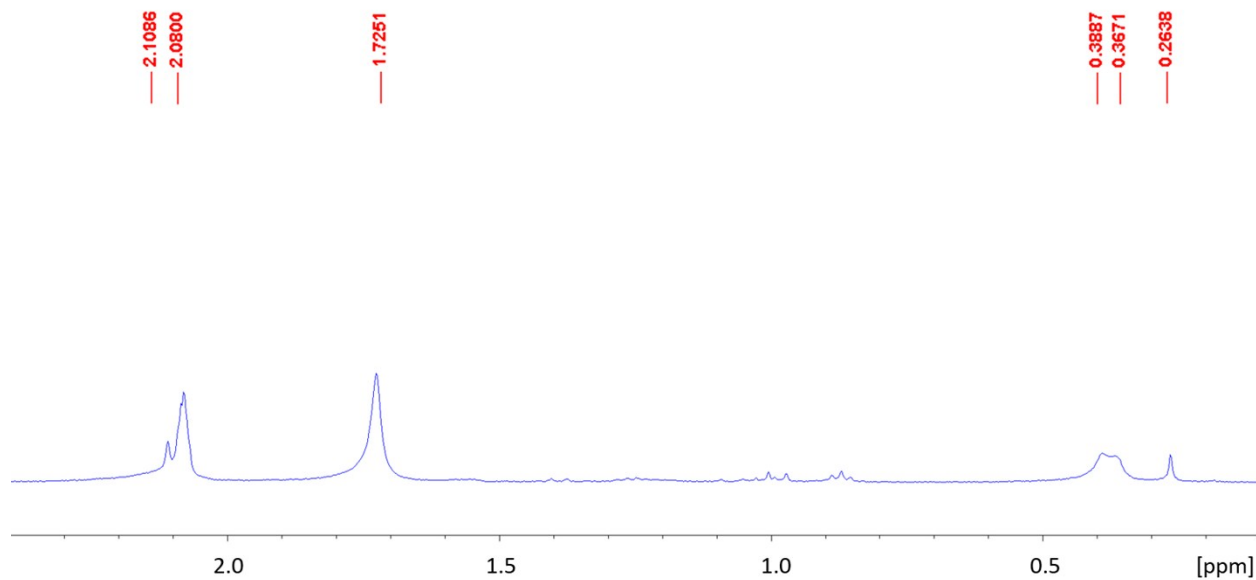


**Figure S2.** <sup>1</sup>H NMR spectrum (<sup>t</sup>Bu region) of U<sub>2</sub>(H<sub>3</sub>BP'Bu<sub>2</sub>BH<sub>3</sub>)<sub>6</sub> (1) in toluene-*d*<sub>8</sub> at 20 °C. Data collected after leaving the crystals under dynamic vacuum overnight to remove solvent in the crystal lattice.

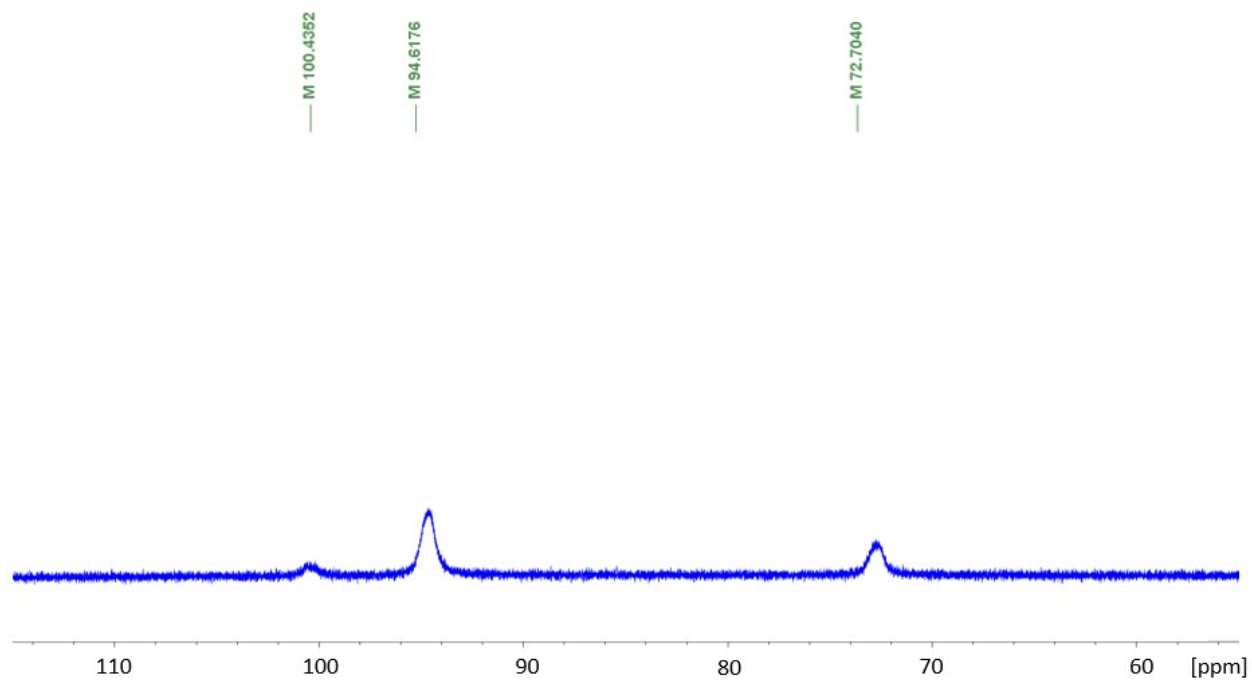


**Figure S3.**  $^1\text{H}$  NMR spectrum ( $\text{BH}_3$  region) of  $\text{U}_2(\text{H}_3\text{BP}'\text{Bu}_2\text{BH}_3)_6$  (**1**) in toluene- $d_8$  at 20 °C.

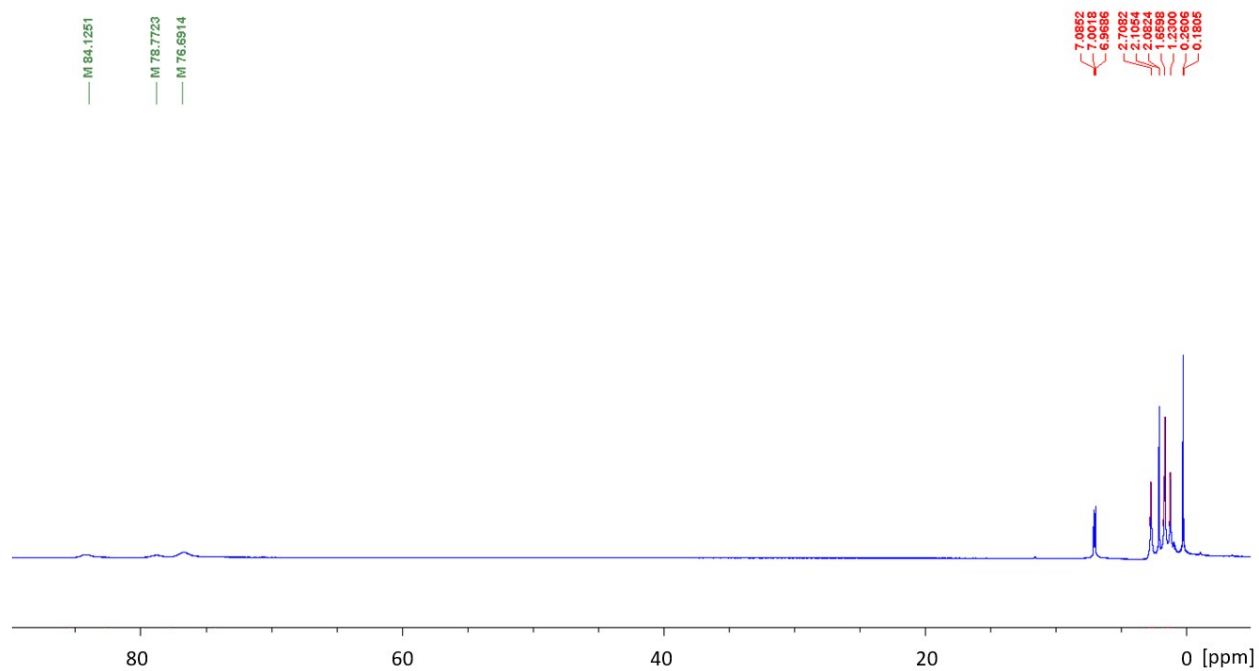


**Figure S4.**  $^1\text{H}$  NMR full spectrum of  $\text{Nd}_2(\text{H}_3\text{BP}'\text{Bu}_2\text{BH}_3)_6$  (**2**) in toluene- $d_8$  at 20 °C. Data collected after leaving the crystals under dynamic vacuum overnight to remove solvent in the crystal lattice.

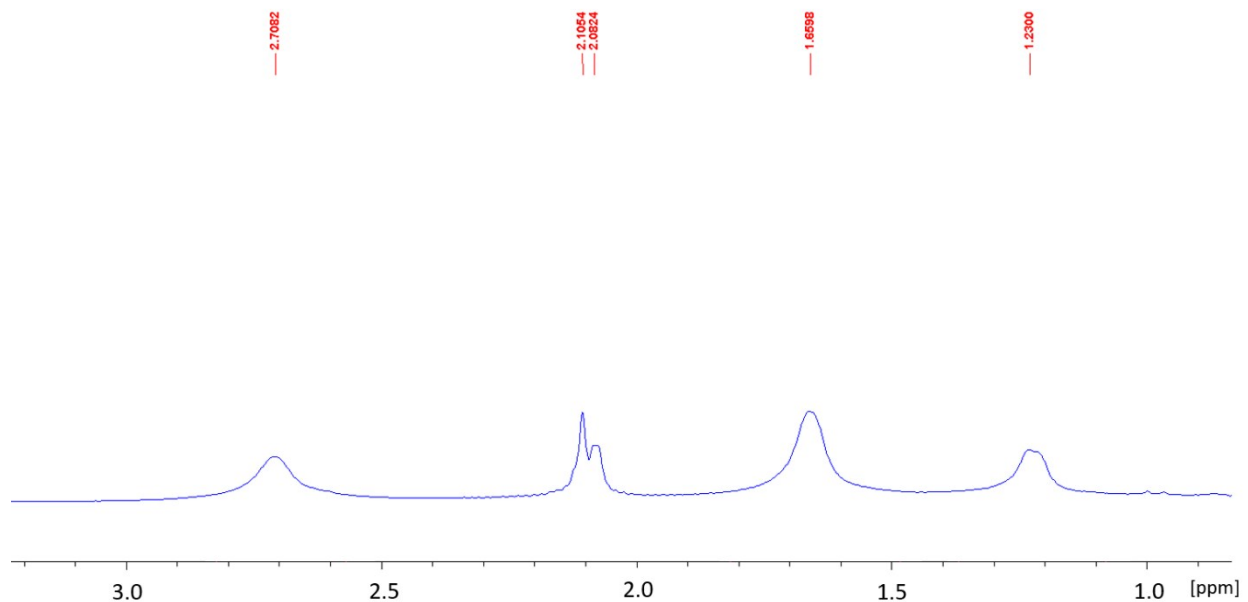


**Figure S5.**  $^1\text{H}$  NMR spectrum ( $t\text{Bu}$  region) of  $\text{Nd}_2(\text{H}_3\text{BP}^t\text{Bu}_2\text{BH}_3)_6$  (**2**) in  $\text{toluene-}d_8$  at  $20\text{ }^\circ\text{C}$ . Data collected after leaving the crystals under dynamic vacuum overnight to remove solvent in the crystal lattice.

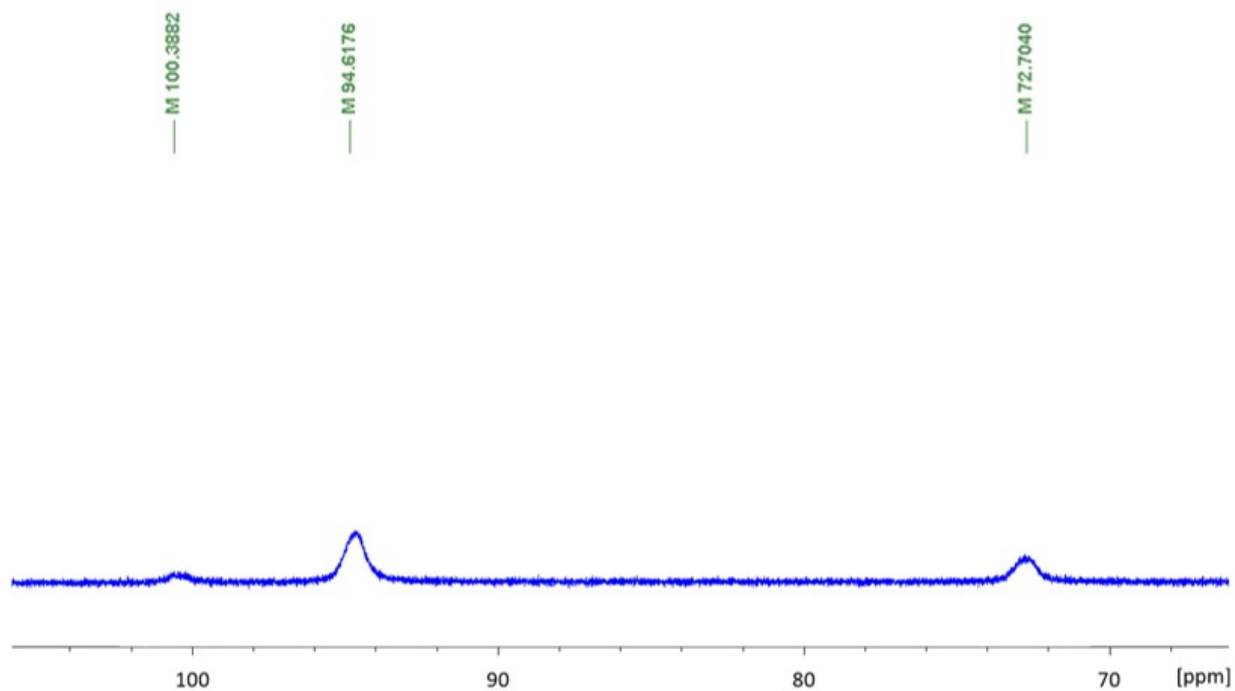


**Figure S6.**  $^1\text{H}$  NMR spectrum ( $\text{BH}_3$  region) of  $\text{Nd}_2(\text{H}_3\text{BP}^t\text{Bu}_2\text{BH}_3)_6$  (**2**) in  $\text{toluene-}d_8$  at  $20\text{ }^\circ\text{C}$ .

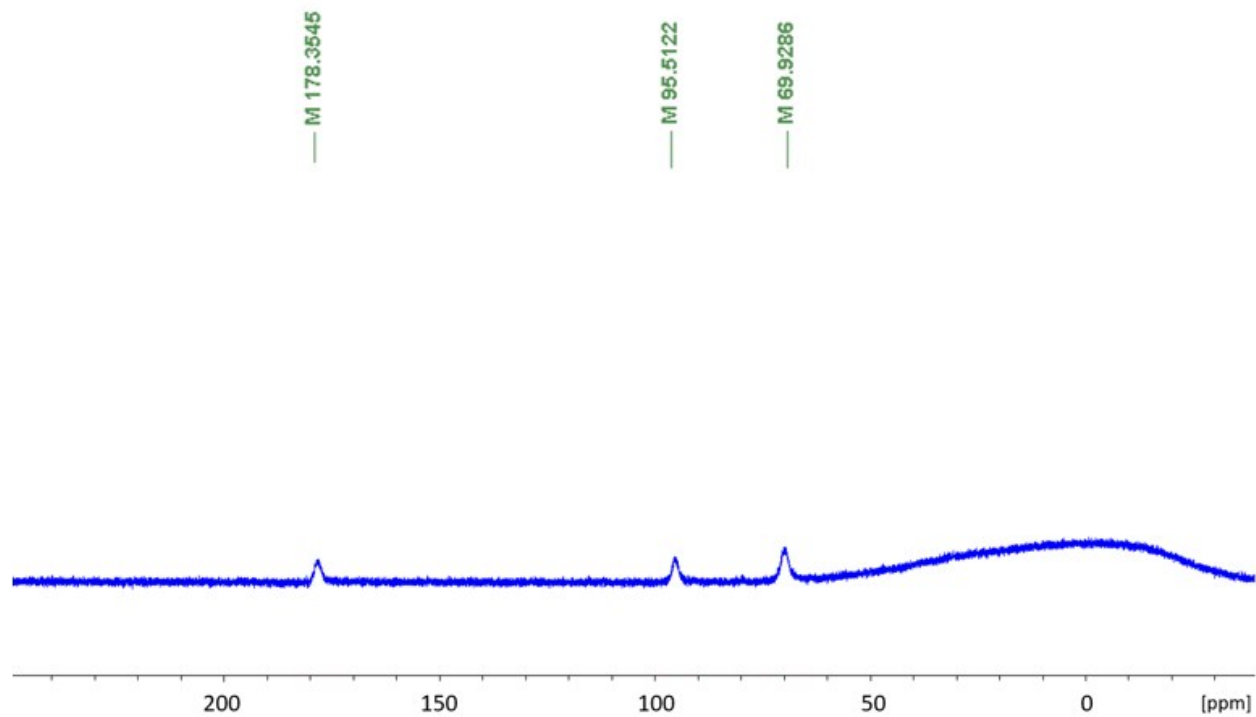


**Figure S7.**  $^{11}\text{B}$  NMR spectrum of  $\text{Nd}_2(\text{H}_3\text{BP}'\text{Bu}_2\text{BH}_3)_6$  (**2**) in  $\text{toluene-}d_8$  at  $20\text{ }^\circ\text{C}$ . The broad peak around  $0\text{ ppm}$  is attributed to background from borosilicate glass in the instrument.

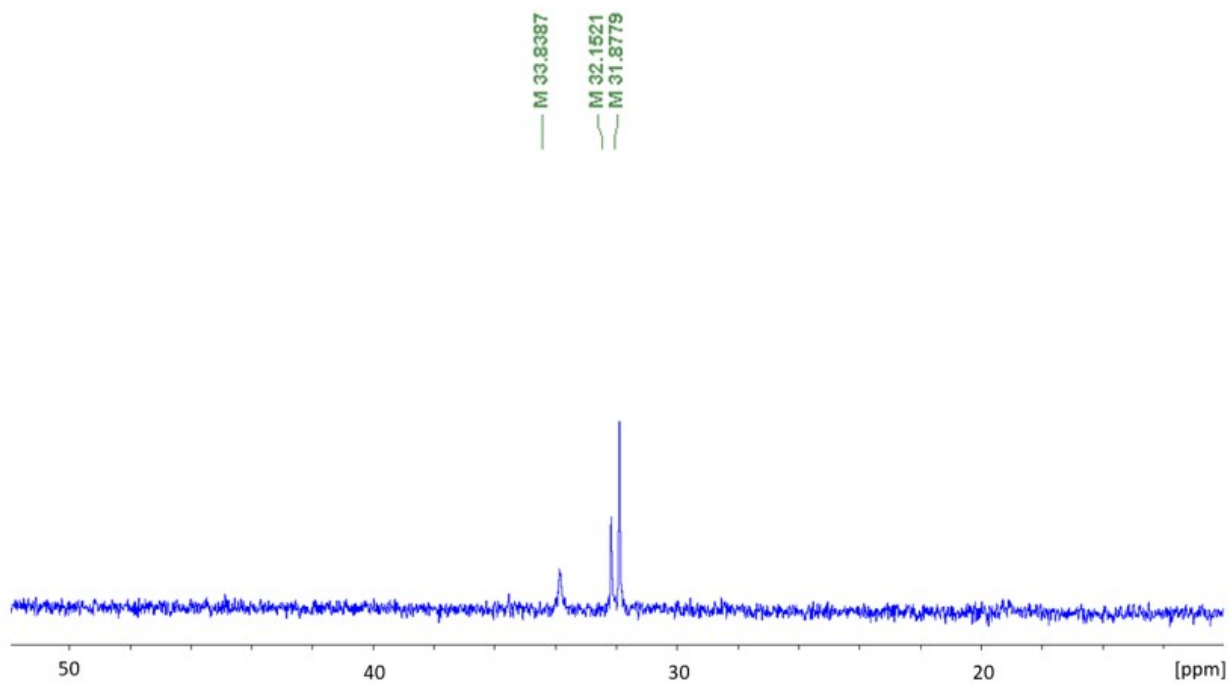


**Figure S8.**  $^{13}\text{C}$  NMR spectrum of  $\text{Nd}_2(\text{H}_3\text{BP}'\text{Bu}_2\text{BH}_3)_6$  (**2**) in  $\text{C}_6\text{D}_6$  at  $20\text{ }^\circ\text{C}$ . Data collected after leaving the crystals under dynamic vacuum overnight to remove solvent in the crystal lattice.

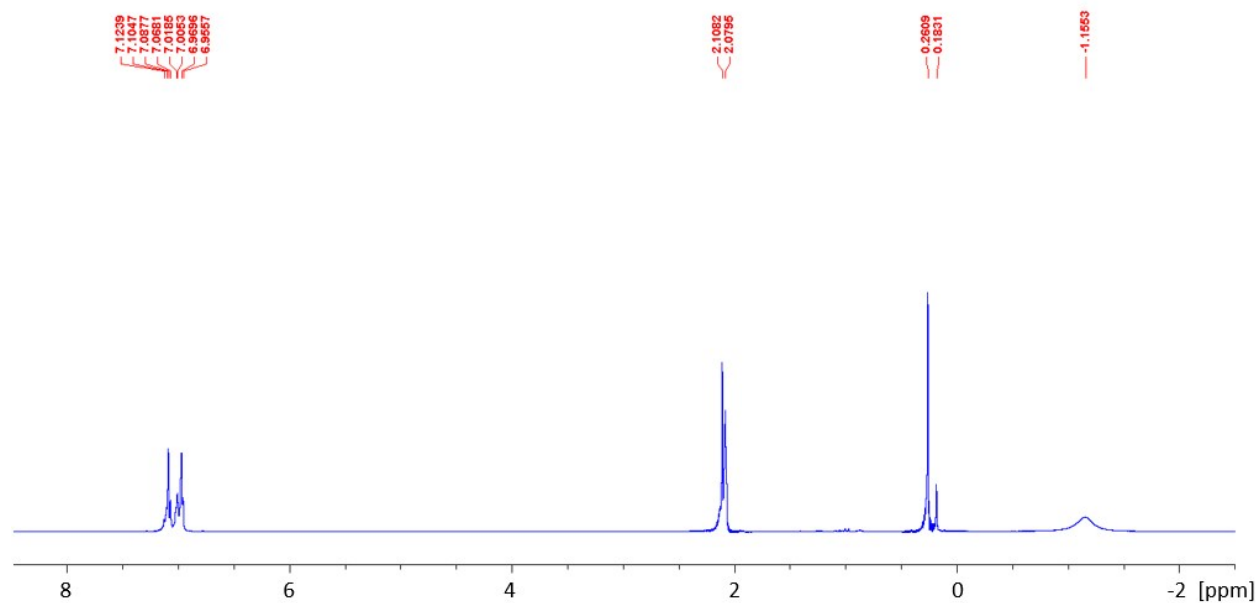


**Figure S9.**  $^1\text{H}$  NMR spectrum ( $t\text{Bu}$  region) of  $\text{Er}_2(\text{H}_3\text{BP}'\text{Bu}_2\text{BH}_3)_6$  (**3**) in toluene- $d_8$  at 20 °C. Data collected after leaving the crystals under dynamic vacuum overnight to remove solvent in the crystal lattice.

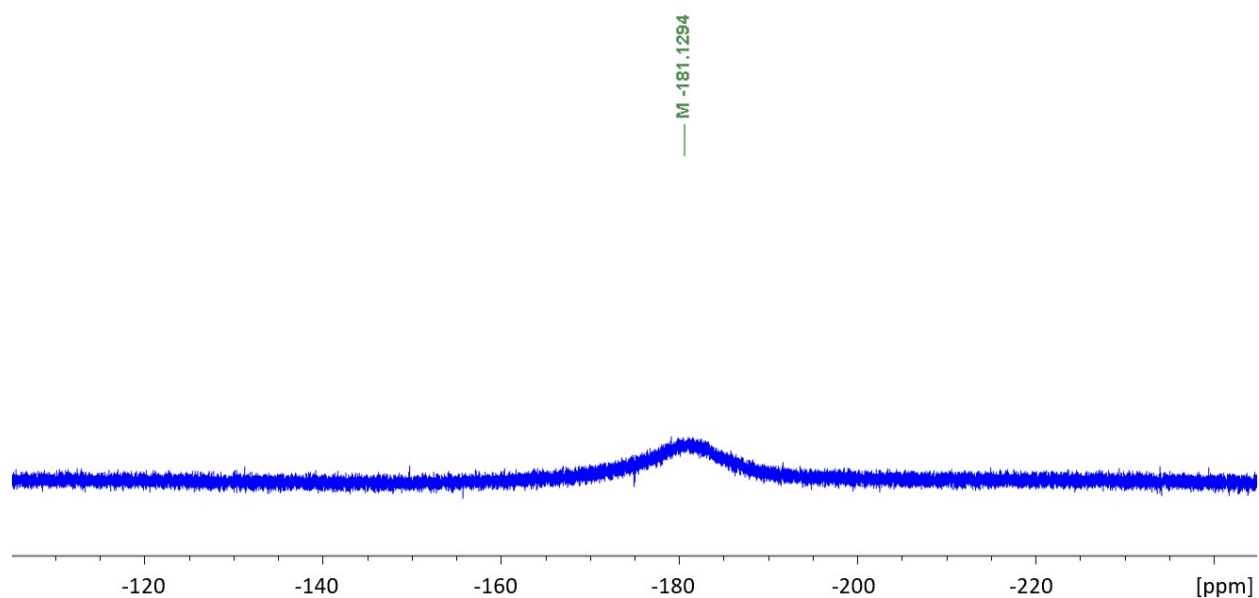


**Figure S10.**  $^1\text{H}$  NMR spectrum ( $\text{BH}_3$  region) of  $\text{Er}_2(\text{H}_3\text{BP}'\text{Bu}_2\text{BH}_3)_6$  (**3**) in toluene- $d_8$  at 20 °C.

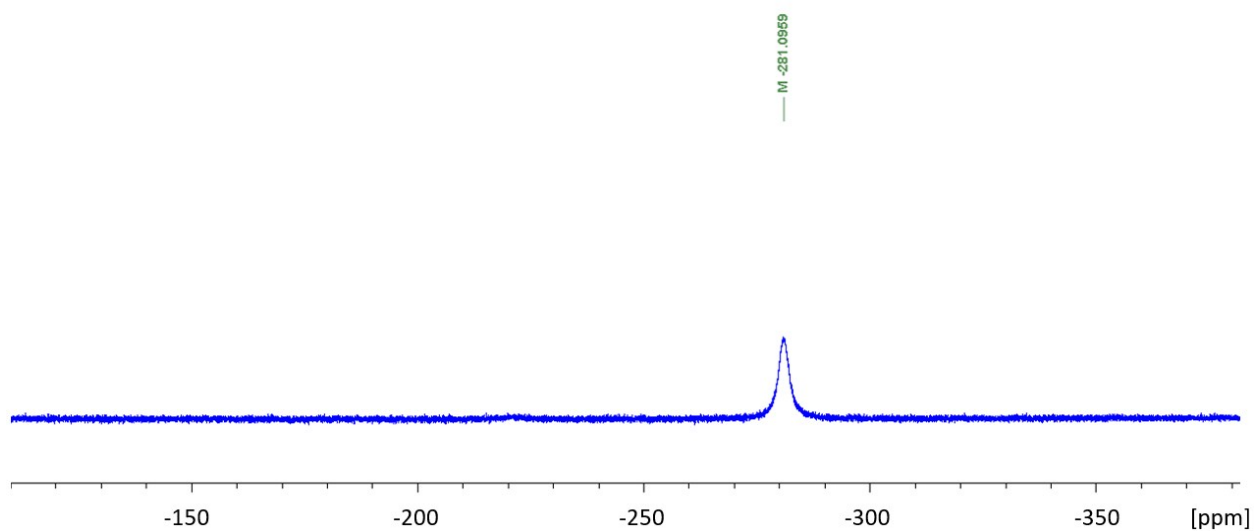


**Figure S11.**  $^{11}\text{B}$  NMR spectrum of  $\text{Er}_2(\text{H}_3\text{BP}'\text{Bu}_2\text{BH}_3)_6$  (**3**) in toluene- $d_8$  at 20 °C.

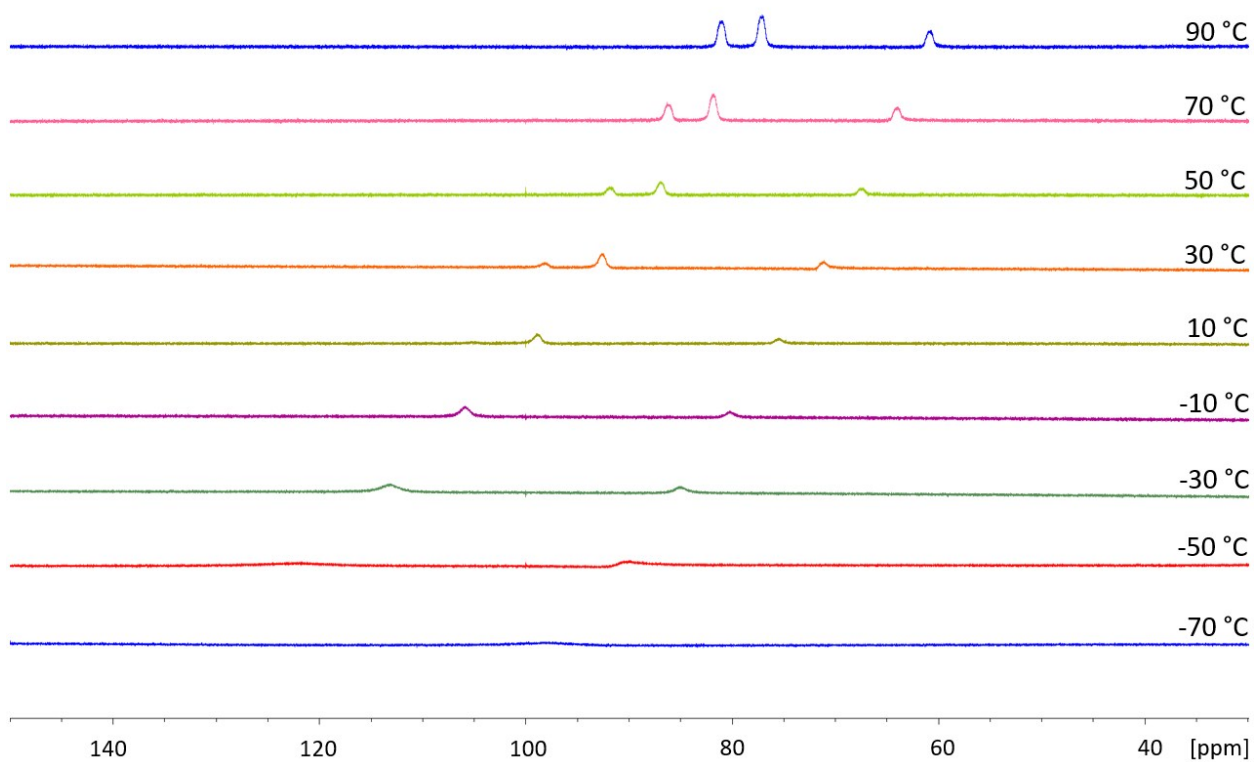


**Figure S12.** Variable temperature  $^1\text{H}$  NMR spectra ( $\text{BH}_3$  region) of  $\text{U}_2(\text{H}_3\text{BP}'\text{Bu}_2\text{BH}_3)_6$  (**1**) in toluene- $d_8$ .

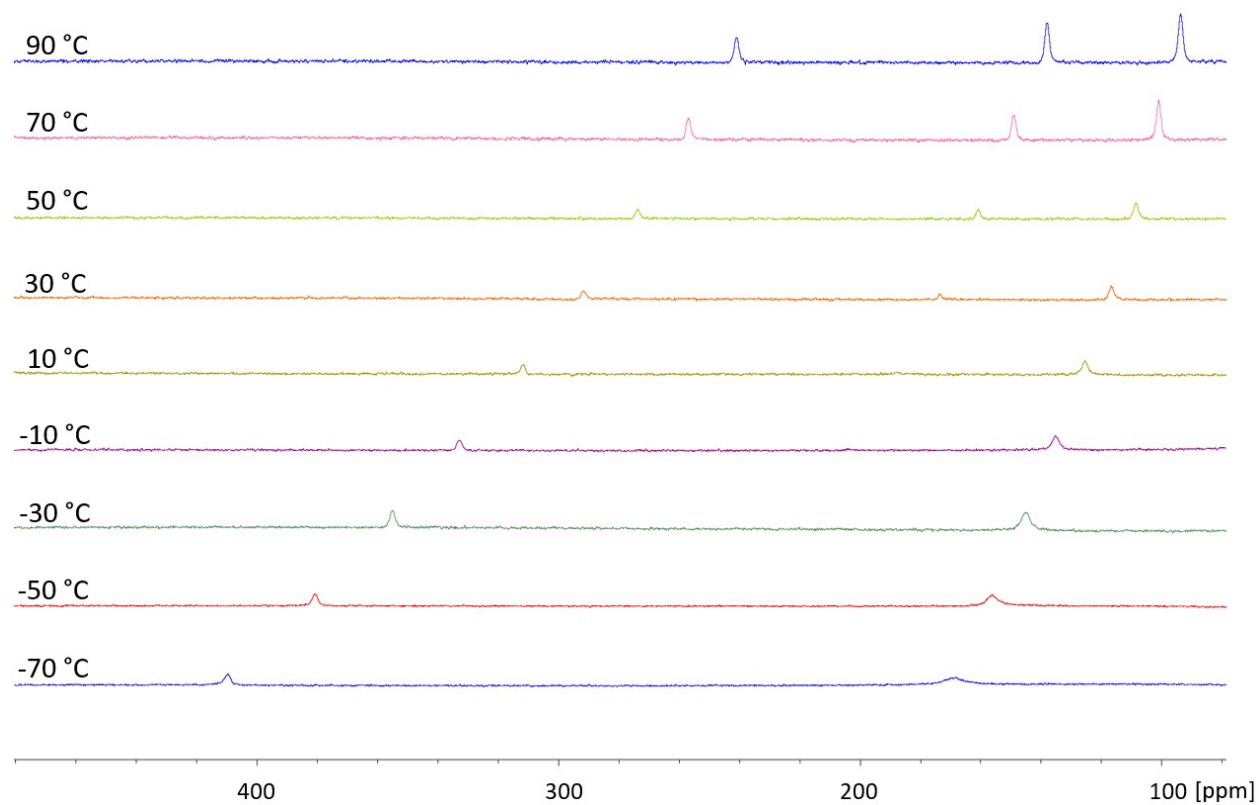


**Figure S13.** Variable-temperature  $^{11}\text{B}$  NMR spectra of  $\text{U}_2(\text{H}_3\text{BP}'\text{Bu}_2\text{BH}_3)_6$  (**1**) in toluene- $d_8$ .

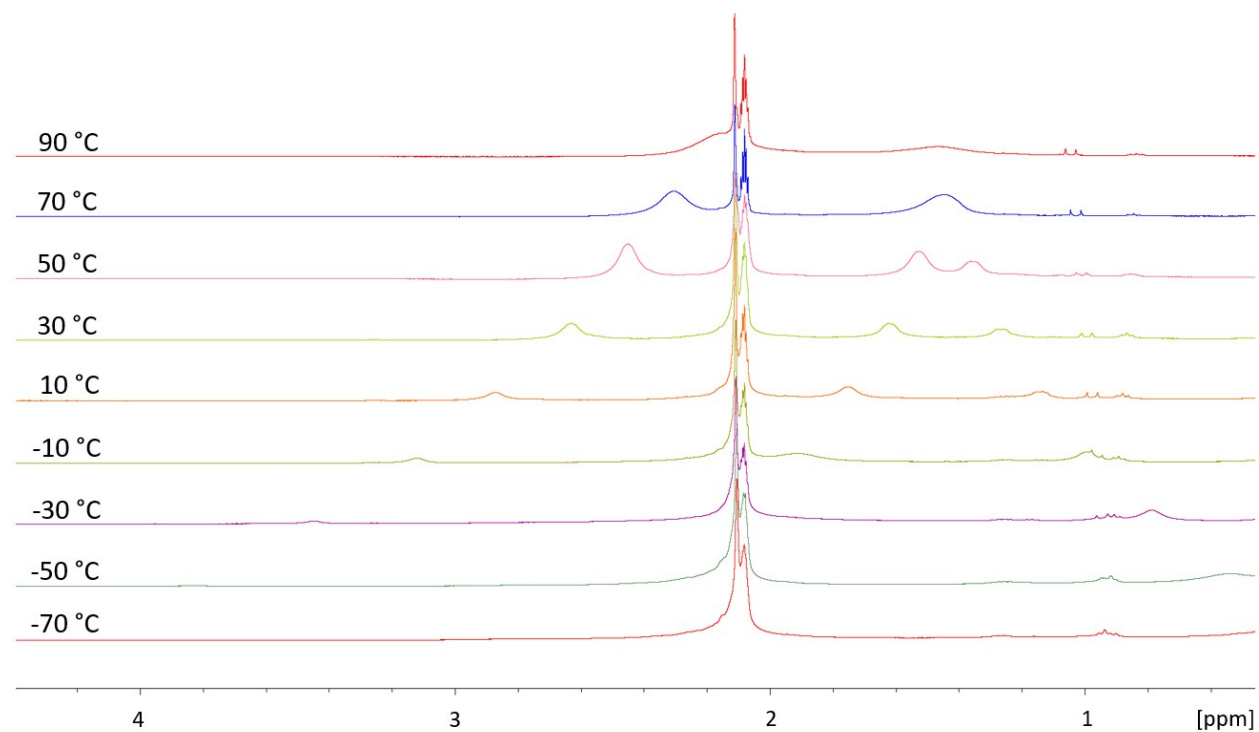


**Figure S14.** Variable temperature  $^1\text{H}$  NMR spectra (tBu region) of  $\text{Nd}_2(\text{H}_3\text{BP}'\text{Bu}_2\text{BH}_3)_6$  (**2**) in toluene- $d_8$ .

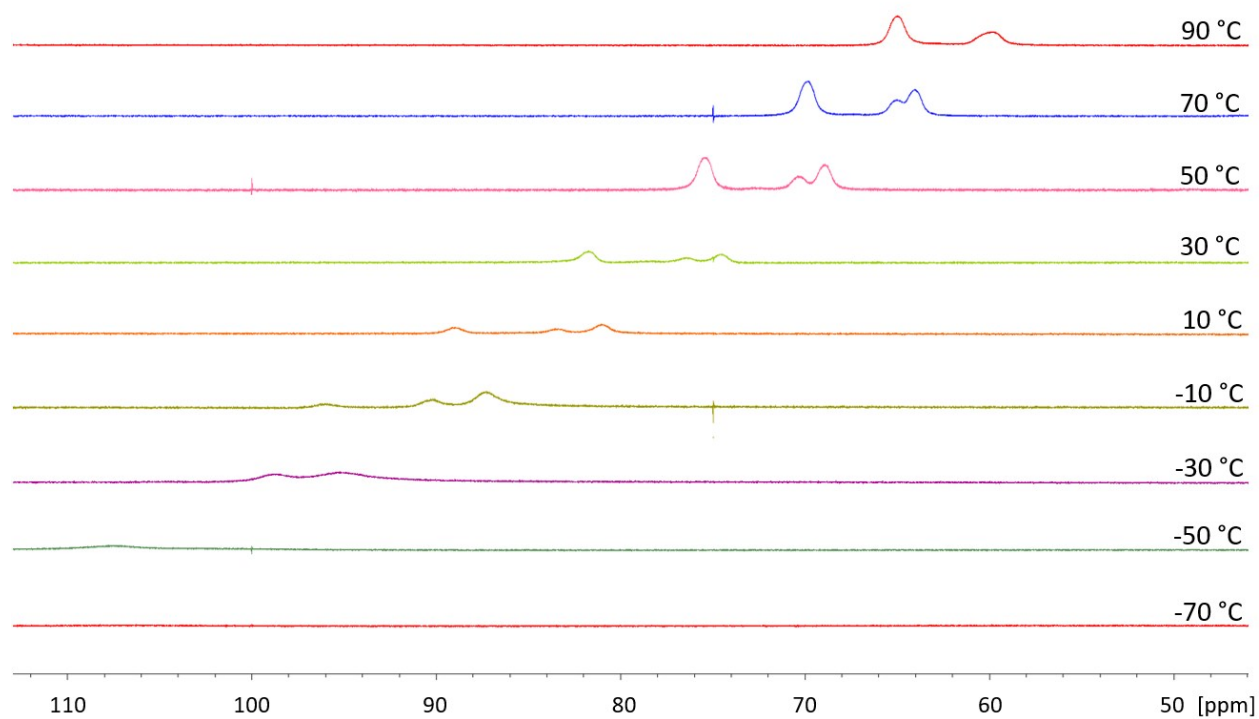


**Figure S15.** Variable temperature  $^1\text{H}$  NMR spectra ( $\text{BH}_3$  region) of  $\text{Nd}_2(\text{H}_3\text{BP}'\text{Bu}_2\text{BH}_3)_6$  (**2**) in toluene- $d_8$ .

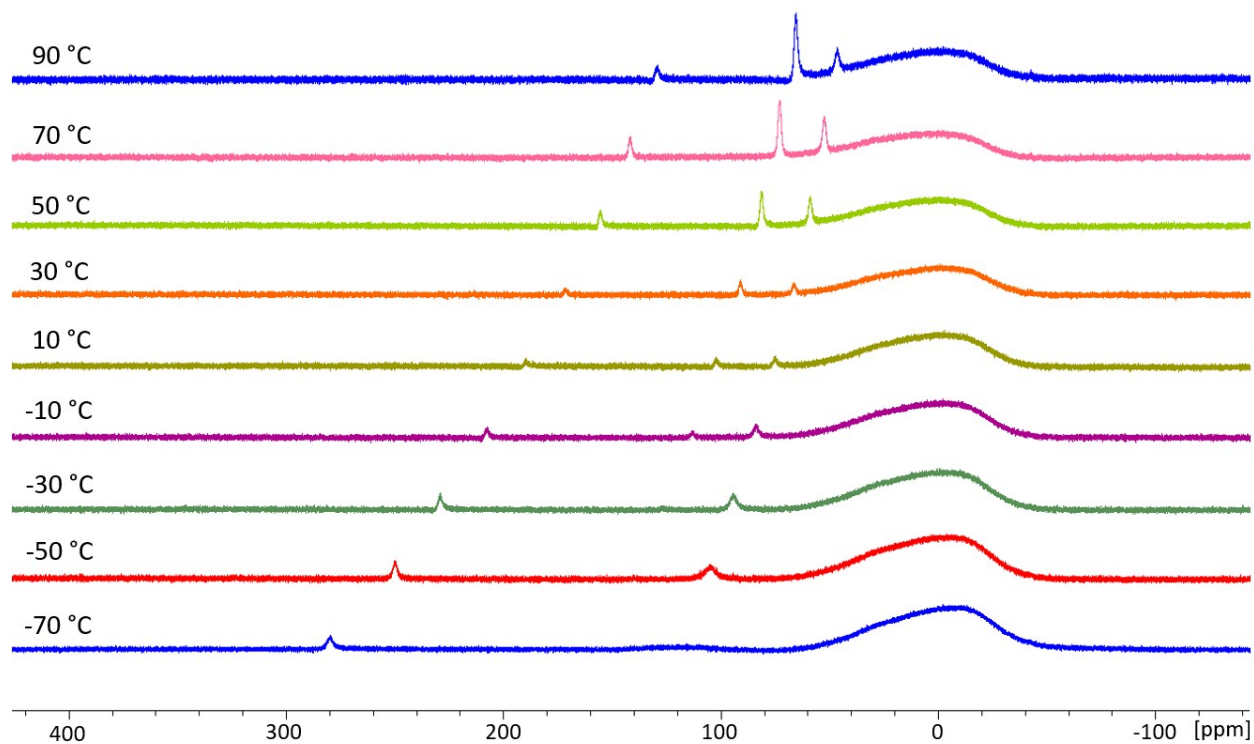


**Figure S16.** Variable-temperature  $^{11}\text{B}$  NMR spectra of  $\text{Nd}_2(\text{H}_3\text{BP}'\text{Bu}_2\text{BH}_3)_6$  (**2**) in toluene- $d_8$ . The broad peak around 0 ppm is attributed to background from borosilicate glass in the instrument.

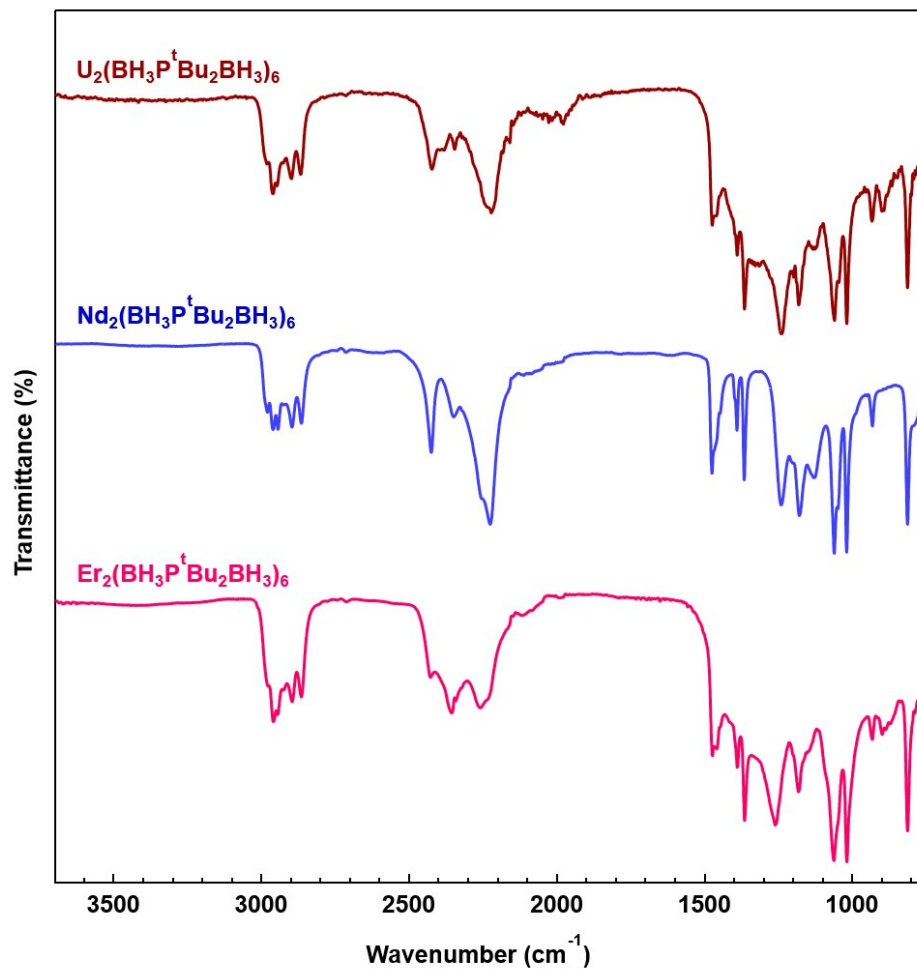


**Figure S17.** Infrared spectra (ATR) of  $\text{U}_2(\text{H}_3\text{BP}^t\text{Bu}_2\text{BH}_3)_6$  (**1**) and  $\text{Nd}_2(\text{H}_3\text{BP}^t\text{Bu}_2\text{BH}_3)_6$  (**2**)  $\text{Er}_2(\text{H}_3\text{BP}^t\text{Bu}_2\text{BH}_3)_6$  (**3**).

## Supporting Information References

- [1] a) M. J. Monreal, R. K. Thomson, T. Cantat, N. E. Travia, B. L. Scott, J. L. Kiplinger, *Organometallics* **2011**, *30*, 2031-2038; b) F. Dornhaus, M. Bolte, *Acta Crystallogr., Sect. E Struct. Rep. Online* **2006**, *62*, m3573-m3575.
- [2] K. Lee, H. Wei, A. V. Blake, C. M. Donahue, J. M. Keith, S. R. Daly, *Dalton Trans.* **2016**, *45*, 9774-9785.
- [3] G. M. Sheldrick, *Acta Crystallogr., Sect. A Found. Crystallogr.* **2008**, *64*, 112-122.
- [4] O. V. Dolomanov, L. J. Bourhis, R. J. Gildea, J. A. K. Howard, H. Puschmann, *J. Appl. Crystallogr.* **2009**, *42*, 339-341.